Open access • Journal Article • DOI:10.1038/NATURE09648

Structure of a nanobody-stabilized active state of the β2 adrenoceptor

Søren G. F. Rasmussen, Hee Jung Choi, Juan Jose Fung, Els Pardon ...+14 more authors

Institutions: Stanford University, Vrije Universiteit Brussel, Boehringer Ingelheim, University of Wisconsin–Milwaukee ...+1 more institutions

Published on: 13 Jan 2011 - Nature (Nature Publishing Group)

Topics: G protein-coupled receptor

Structure of a nanobody-stabilized active state of the b2 adrenoceptor

Rasmussen, Soren G. F.; Choi, Hee-Jung; Fung, Juan Jose; Pardon, Els; Casarosa, Paola; Chae, Pil Seok; Devree, Brian T.; Rosenbaum, Daniel M.; Thian, Foon Sun; Kobilka, Tong Sun; Schnapp, Andreas; Konetzki, Ingo; Sunahara, Roger K.; Gellman, Samuel H.; Pautsch, Alexander; Steyaert, Jan; Weis, William I.; Kobilka, Brian K

Published in:
Nature

DOI:
10.1038/nature09648

Publication date:
2011

Document Version:
Final published version

ARTICLE

doi:10.1038/nature09648

Structure of a nanobody–stabilized active state of the β_2 adrenoceptor

Søren G. F. Rasmussen[1,2]*, Hee-Jung Choi[1,3]*, Juan Jose Fung[1]*, Els Pardon[4,5], Paola Casarosa[6], Pil Seok Chae[7], Brian T. DeVree[8], Daniel M. Rosenbaum[1], Foon Sun Thian[1], Tong Sun Kobilka[1], Andreas Schnapp[6], Ingo Konetzki[6], Roger K. Sunahara[8], Samuel H. Gellman[7], Alexander Pautsch[6], Jan Steyaert[4,5], William I. Weis[1,3] & Brian K. Kobilka[1]

G protein coupled receptors (GPCRs) exhibit a spectrum of functional behaviours in response to natural and synthetic ligands. Recent crystal structures provide insights into inactive states of several GPCRs. Efforts to obtain an agonist–bound active–state GPCR structure have proven difficult due to the inherent instability of this state in the absence of a G protein. We generated a camelid antibody fragment (nanobody) to the human β_2 adrenergic receptor (β_2AR) that exhibits G protein–like behaviour, and obtained an agonist–bound, active–state crystal structure of the receptor–nanobody complex. Comparison with the inactive β_2AR structure reveals subtle changes in the binding pocket; however, these small changes are associated with an 11 Å outward movement of the cytoplasmic end of transmembrane segment 6, and rearrangements of transmembrane segments 5 and 7 that are remarkably similar to those observed in opsin, an active form of rhodopsin. This structure provides insights into the process of agonist binding and activation.

GPCRs activated by diffusible ligands have a spectrum of functional states[1]. A GPCR may activate more than one G protein isoform or a G-protein-independent pathway such as arrestin. In the absence of a ligand, many GPCRs exhibit some basal, agonist independent activity towards one or more of these signalling pathways. Orthosteric ligands (compounds that occupy the native hormone-binding pocket) are classified according to their efficacy, that is, the effect that they have on receptor signalling through a specific pathway. Inverse agonists inhibit basal activity whereas agonists maximally activate the receptor. Partial agonists induce submaximal activity, even at saturating concentrations. Neutral antagonists have no effect on basal activity, but sterically block the activity of other ligands. Moreover, the efficacy profile of ligands for a given GPCR can differ for different downstream signalling pathways. The presence of some activity in the unliganded receptor implies low energy barriers between functional states, such that thermal fluctuations significantly sample activating conformations, and ligands with distinct efficacy profiles act by stabilizing distinct subsets of conformations.

We know little about the structural basis for the functional versatility of GPCRs. Only rhodopsin has been crystallized in different conformational states[2–5]. The first structures of rhodopsin covalently bound to 11-*cis*-retinal represent a completely inactive state with virtually no basal activity[5]. Structures of opsin, the ligand-free form of rhodopsin, obtained from crystals grown at pH 5.6 are likely to represent active conformations[2,3], as the Fourier transform infrared (FTIR) spectrum of opsin at acidic pH resembles that of metarhodopsin II, the light-activated form of rhodopsin[6]. For rhodopsin, the light-induced transition from the inactive to the active state is very efficient. Rhodopsin is activated by photoisomerization of a covalent ligand, with efficient transfer of energy from the absorbed photon to the receptor. Crystal structures of low-pH opsin reveal that the protein conformation is the same in the presence or absence of a peptide from the alpha subunit of transducin (Gt), its cognate G protein, consistent with the notion that metarhodopsin II can adopt a fully active conformation in the absence of Gt.

The crystal structures of GPCRs activated by diffusible ligands, including the human β_2AR[7–10], the avian β_1AR[11], and the human adenosine A_{2A} receptor[12], represent inactive conformations bound by inverse agonists. Unlike the activation of rhodopsin by light, agonists are much less efficient at stabilizing the active state of the β_2AR, making it difficult to capture this state in a crystal structure. Fluorescence lifetime studies show that even saturating concentrations of the full agonist isoproterenol do not stabilize a single active conformation[13]. This may be due to the relatively low affinity and rapid rates of association and dissociation for β_2AR agonists. However, in a companion manuscript we show that, even when bound to a covalent agonist, the β_2AR crystallizes in an inactive conformation[14]. Experiments using a β_2AR labelled with a conformationally sensitive fluorescent probe show that stabilization of the active state requires both agonist and Gs, the stimulatory G protein for adenylyl cyclase[15]. Efforts to obtain an agonist-GPCR-G protein complex are of great importance; however, this is a particularly difficult endeavour due to the biochemical challenges in working with both GPCRs and G proteins, and the inherent instability of the complex in detergent solutions. As an alternate approach, we developed a binding protein that preferentially binds to and stabilizes an active conformation, acting as a surrogate for Gs.

Nanobody–stabilized β_2AR active state

The active G protein coupled state of the β_2AR (and many other family A GPCRs) has characteristic functional properties. Agonists promote Gs binding to the β_2AR and G protein binding to the receptor increases agonist affinity. We identified a camelid antibody fragment

[1]Department of Molecular and Cellular Physiology, Stanford University School of Medicine, 279 Campus Drive, Stanford, California 94305, USA. [2]Department of Neuroscience and Pharmacology, The Panum Institute, University of Copenhagen, Blegdamsvej 3, 2200 Copenhagen N, Denmark. [3]Department of Structural Biology, Stanford University School of Medicine, 299 Campus Drive, Stanford, California 94305, USA. [4]Department of Molecular and Cellular Interactions, Vlaams Instituut voor Biotechnologie (VIB), Vrije Universiteit Brussel, B-1050 Brussels, Belgium. [5]Structural Biology Brussels, Vrije Universiteit Brussel, B-1050 Brussels, Belgium. [6]Boehringer Ingelheim Pharma GmbH & Co. KG, Germany. [7]Department of Chemistry, University of Wisconsin, Madison, Wisconsin 53706, USA. [8]Department of Pharmacology, University of Michigan Medical School, Ann Arbor, Michigan 48109, USA.
*These authors contributed equally to this work.

that exhibits G protein-like behaviour towards the β_2AR. Tylopoda (camels, dromedaries and llamas) have developed a unique class of functional antibody molecules that are devoid of light chains[16]. A nanobody (Nb) is the recombinant minimal-sized intact antigen-binding domain of such a camelid heavy chain antibody and is approximately 25% the size of a conventional Fab fragment. To generate receptor-specific nanobodies, a llama was immunized with purified agonist-bound β_2AR reconstituted at high density into phospholipid vesicles. A library of single-chain nanobody clones was generated and screened against agonist bound receptor. We identified seven clones that recognized agonist-bound β_2AR. Of these, Nb80 was chosen because it showed G-protein-like properties upon binding to both wild-type β_2AR and β_2AR–T4L, the β_2AR–T4 lysozyme fusion protein used to obtain the high-resolution inactive state crystal structure[7,9].

We compared the effect of Nb80 with Gs on β_2AR structure and agonist binding affinity. β_2AR was labelled at the cytoplasmic end of transmembrane helix 6 (TM6) at Cys 265 with the fluorophore monobromobimane and reconstituted into high-density lipoprotein (HDL) particles. TM6 moves relative to TM3 and TM5 upon agonist activation (Fig. 1a), and we have shown previously that the environment around bimane covalently linked to Cys 265 changes with both agonist binding and G protein coupling, resulting in a decrease in fluorescence intensity and a red shift in λ_{max}[15]. As shown in Fig. 1b, the catecholamine agonist isoproterenol and Gs both stabilize an active-like conformation, but the effect of Gs is greater in the presence of isoproterenol, consistent with the cooperative interactions of agonist and Gs on β_2AR structure. Nb80 alone has an effect on bimane fluorescence and λ_{max} of unliganded β_2AR that is similar to that of Gs (Fig. 1c). This effect was not observed in β_2AR bound to the inverse agonist ICI-118,551. The effect of Nb80 was increased in the presence of 10 μM isoproterenol. These results show that Nb80 does not recognize the inactive conformation of the β_2AR, but binds efficiently to agonist-occupied β_2AR and produces a change in bimane fluorescence that is indistinguishable from that observed in the presence of Gs and isoproterenol.

Figure 1d and e shows the effect of Gs and Nb80 on agonist affinity for β_2AR. β_2AR was reconstituted into HDL particles and agonist competition binding experiments were performed in the absence or presence of Nb80 and Gs. In the absence of either protein, isoproterenol has an inhibition constant (K_i) of 107 nM. In the presence of Gs two affinity states are observed, because not all of the β_2AR is coupled to Gs. In the Gs-coupled state the affinity of isoproterenol increases by 100-fold (K_i = 1.07 nM) (Fig. 1d and Supplementary Table 1). Similarly, in the presence of Nb80 the affinity of isoproterenol increases by 95-fold (K_i = 1.13 nM) (Fig. 1e and Supplementary Table 1). In contrast, Nb80 had little effect on β_2AR binding to the inverse agonist ICI-118,551 (Supplementary Fig. 1 and Supplementary Table 1). These binding data indicate that Nb80 stabilizes a conformation in wild-type β_2AR that is very similar to that stabilized by Gs, such that the energetic coupling of agonist and Gs binding is faithfully mimicked by Nb80.

The high-resolution structure of the inactive state of the β_2AR was obtained with a β_2AR–T4L fusion protein. We showed previously that β_2AR–T4L has a higher affinity for isoproterenol than wild-type β_2AR[7]. Nevertheless, in the presence of Nb80 the affinity increased by 60-fold, resulting in an affinity (K_i = 0.56 nM) comparable to that of wild-type β_2AR bound to Nb80 (Fig. 1f and Supplementary Table 1). Although we cannot study G protein coupling in β_2AR–T4L due to steric hindrance by T4L, the results show that T4L does not prevent binding of Nb80, and the nearly identical K_i values for agonist binding to wild-type β_2AR and β_2AR–T4L in the presence of Nb80 indicate that Nb80 stabilizes a similar conformation in these two proteins. The most likely explanation for the ability of Nb80 to bind to β_2AR–T4L whereas Gs does not is the difference in size of these two proteins. Nb80 is approximately 14 kDa whereas the Gs heterotrimer is approximately 90 kDa.

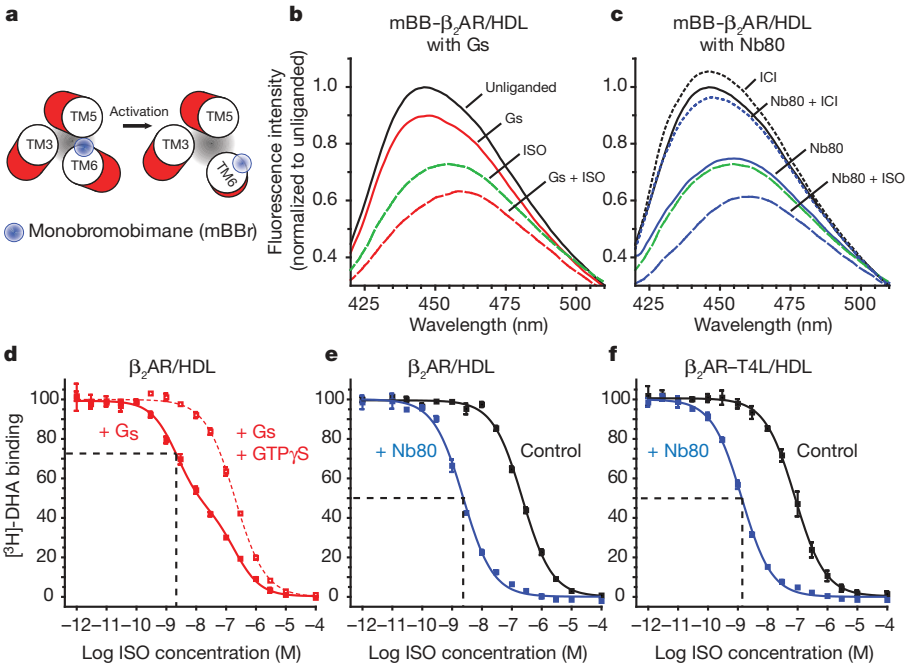

Figure 1 | Effect of Nb80 on β_2AR structure and function. **a**, The cartoon illustrates the movement of the environmentally-sensitive bimane probe attached to Cys $265^{6.27}$ in the cytoplasmic end of TM6 from a more buried, hydrophobic environment to a more polar, solvent-exposed position during receptor activation that results in a decrease in fluorescence in Fig. 1b–c and Supplementary Fig. 2c, d. **b**, **c**, Fluorescence emission spectra showing ligand-induced conformational changes of monobromobimane-labelled β_2AR reconstituted into high density lipoprotein particles (mBB-β_2AR/HDL) in the absence (black solid line) or presence of full agonist isoproterenol (ISO, green wide dashed line), inverse agonist ICI-118,551 (ICI, black dashed line), Gs heterotrimer (red solid line), nanobody-80 (Nb80, blue solid lines), and combinations of Gs with ISO (red wide dashed line), Nb80 with ISO (blue wide dashed line), and Nb80 with ICI (blue dashed line). **d**–**f**, Ligand binding curves for ISO competing against [^{3}H]-dihydroalprenolol ([^{3}H]-DHA) for **d**, β_2AR/HDL reconstituted with Gs heterotrimer in the absence or presence GTPγS; **e**, β_2AR/HDL in the absence and presence of Nb80; and **f**, β_2AR–T4L/HDL in the absence and presence of Nb80. Error bars represent standard errors.

High affinity β_2AR agonist

To stabilize further the active state of the β_2AR, we screened over 50 commercial and proprietary β_2AR ligands. Of these, BI-167107 (Boehringer Ingelheim) had the most favourable efficacy, affinity and off-rate profile. BI-167107 is a full agonist that binds to the β_2AR with a dissociation constant K_d of 84 pM (Supplementary Fig. 2a and b). As shown in Supplementary Fig. 2c and d, BI-167107 induces a larger change in the fluorescence intensity and λ_{max} of bimane bound to Cys 265 than does the agonist isoproterenol. Moreover, the rate of dissociation of BI-167107 was extremely slow. Displacement of BI-167107 with an excess of the neutral antagonist alprenolol required 150 h to complete, compared with 5 s for isoproterenol.

Crystallization of β_2AR–T4L–Nb80 complex

The β_2AR was originally crystallized bound to the inverse agonist carazolol using two different approaches. The first crystals were obtained from β_2AR bound to a Fab fragment that recognized an epitope composed of the amino and carboxyl terminal ends of the third intracellular loop connecting TMs 5 and 6 (ref. 8). In the second approach, the third intracellular loop was replaced by T4 lysozyme (β_2AR–T4L)[7]. Efforts to crystallize β_2AR–Fab complex and β_2AR–T4L bound to BI-167107 and other agonists failed to produce crystals of sufficient quality for structure determination. We therefore attempted to crystallize BI-167107 bound to β_2AR and β_2AR–T4L in complex with Nb80. Although crystals of both complexes were obtained in lipid bicelles and lipidic cubic phase (LCP), high-resolution diffraction was only obtained from crystals of β_2AR–T4L–Nb80 grown in LCP. These crystals grew at pH 8.0 in 39–44% PEG400, 100 mM Tris, 4% DMSO and 1% 1,2,3-heptanetriol.

A merged data set at 3.5 Å was obtained from 23 crystals (Supplementary Table 2). The structure was solved by molecular replacement using the structure of the carazolol-bound β_2AR and a nanobody as search models. Supplementary Fig. 3a shows the packing of the β_2AR–T4L–Nb80 complex in the crystal lattice. The receptor has interactions with lattice neighbours in several directions, and is relatively well ordered (Supplementary Fig. 3a and b), with readily interpretable electron density for most of the polypeptide. Nb80 binds to the cytoplasmic end of the β_2AR, with the third complementarity-determining region (CDR) loop projecting into the core of the receptor (Fig. 2a, and Supplementary Fig. 4).

Agonist-stabilized changes in the β_2AR

Figure 2 b–d compares the inactive β_2AR structure (from the carazolol bound β_2AR–T4L structure) with the agonist-bound β_2AR component of the β_2AR–T4L–Nb80 complex. The largest differences are found at the cytoplasmic face of the receptor, with outward displacement of TM5 and TM6 and an inward movement of TM7 and TM3 in the β_2AR–T4L–Nb80 complex relative to the inactive structure. There

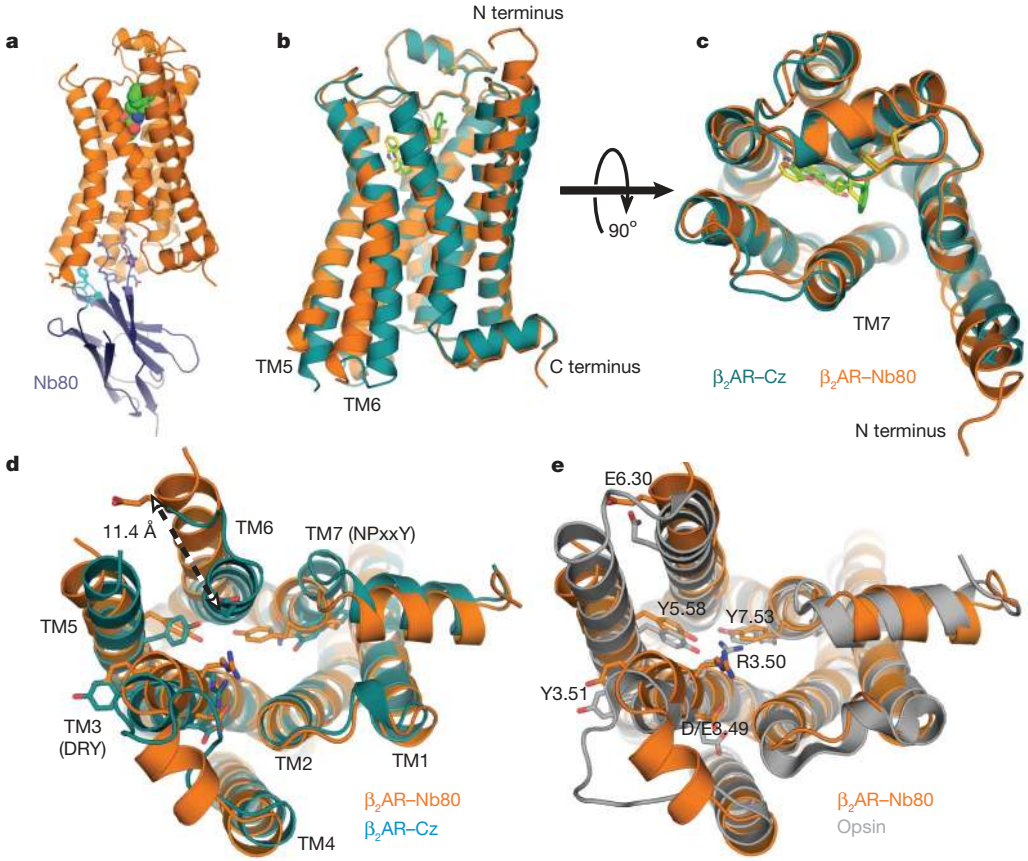

Figure 2 | Comparison of the agonist-Nb80 stabilized crystal structures of the β_2AR with inverse agonist bound β_2AR and opsin. The structure of inverse agonist carazolol-bound β_2AR–T4L (β_2AR–Cz) is shown in blue with the carazolol in yellow. The structure of BI-167107 agonist-bound and Nb80-stabilized β_2AR–T4L (β_2AR–Nb80) is shown in orange with BI-167107 in green. These two structures were aligned using the PyMOL align function. **a**, Side view of the β_2AR–Nb80 complex with β_2AR in orange and CDRs of Nb80 in light blue (CDR1) and blue (CDR3). **b**, Side view of the superimposed structures showing significant structural changes in the intracellular and G protein facing part of the receptors. **c**, Comparison of the extracellular ligand binding domains showing modest structural changes. **d**, Cytoplasmic view showing the ionic lock interaction between Asp 3.49 and Arg 3.50 of the DRY motif in TM3 is broken in the β_2AR–Nb80 structure. The intracellular end of TM6 is moved outward and away from the core of the receptor. The arrow indicates an 11.4 Å change in distance between the α-carbon of Glu 6.30 in the structures of β_2AR–Cz and β_2AR–Nb80. The intracellular ends of TM3 and TM7 move towards the core by 4 and 2.5 Å, respectively, while TM5 moves outward by 6 Å. **e**, The β_2AR–Nb80 structure superimposed with the structure of opsin crystallized with the C-terminal peptide of Gt (transducin)[2]. PyMOL (http://www.pymol.org) was used for the preparation of all structure figures.

are relatively small changes in the extracellular surface (Fig. 2c). The second intracellular loop (ICL2) between TM3 and TM4 adopts a two-turn alpha helix (Fig. 2d), similar to that observed in the turkey β_1AR structure[11]. The absence of this helix in the inactive β_2AR structure may reflect crystal lattice contacts involving ICL2.

Figure 2a and Supplementary Fig. 4a–c show details of interaction of Nb80 with the cytoplasmic side of the β_2AR. An eight-amino-acid sequence of CDR3 penetrates into a hydrophobic pocket formed by amino acids from TM segments 3, 5, 6 and 7. A four-amino-acid sequence of CDR1 provides additional stabilizing interactions with cytoplasmic ends of TM segments 5 and 6. CDR3 occupies a position similar to the carboxyl terminal peptide of transducin in opsin[2] (Supplementary Fig. 4c, d). The majority of interactions between Nb80 and the β_2AR are mediated by hydrophobic contacts.

When comparing the agonist- and inverse agonist-bound structures, the largest change is observed in TM6, with an 11.4-Å movement of the helix at Glu 268$^{6.30}$ (part of the ionic lock) (superscripts in this form indicate Ballesteros–Weinstein numbering for conserved GPCR residues[17]) (Fig. 2d). This large change is effected by a small clockwise rotation of TM6 in the turn preceding the conserved Pro 288$^{6.50}$, enabled by the interrupted backbone hydrogen bonding at the proline and repacking of Phe 282$^{6.44}$ (see below), which swings the helix outward.

The changes in agonist-bound β_2AR–T4L–Nb80 relative to the inactive carazolol-bound β_2AR–T4L are remarkably similar to those observed between rhodopsin and opsin[2,3] (Fig. 2e). The salt bridge in the ionic lock between highly conserved Arg 131$^{3.50}$ and Asp/Glu 130$^{3.49}$ is broken. In opsin, Arg 135$^{3.50}$ interacts with Tyr 223$^{5.58}$ in TM5 and a backbone carbonyl of the transducin peptide. Arg 131$^{3.50}$ of β_2AR likewise interacts with a backbone carbonyl of CDR3 of Nb80. However, Nb80 precludes an interaction between Arg 131$^{3.50}$ and Tyr 219$^{5.58}$, even though the tyrosine occupies a similar position in opsin and agonist-bound β_2AR–T4L–Nb80. As in opsin, Tyr 326$^{7.53}$ of the highly conserved NPxxY sequence moves into the space occupied by TM6 in the inactive state. In carazolol-bound β_2AR–T4L we observed a network of hydrogen bonding interactions involving highly conserved amino acids in TMs 1, 2, 6 and 7 and several water molecules[7]. Although the resolution of the β_2AR–T4L–Nb80 structure is inadequate to detect water molecules, it is clear that the structural changes we observe would substantially alter this network.

In contrast to the relatively large changes observed in the cytoplasmic domains of β_2AR–T4L–Nb80, the changes in the agonist-binding pocket are fairly subtle. Figure 3 shows a comparison of the binding pockets of the inverse agonist- and agonist-bound structures. An omit map of the ligand-binding pocket is provided in Supplementary Fig. 5. Many of the interactions between the agonist BI-167107 and the β_2AR are similar to those observed with the inverse agonist carazolol. The alkylamine and the β-OH of both ligands form polar interactions with Asp 113$^{3.32}$ in TM3, and with Asn 312$^{7.39}$ and Tyr 316$^{7.43}$ in TM7. The

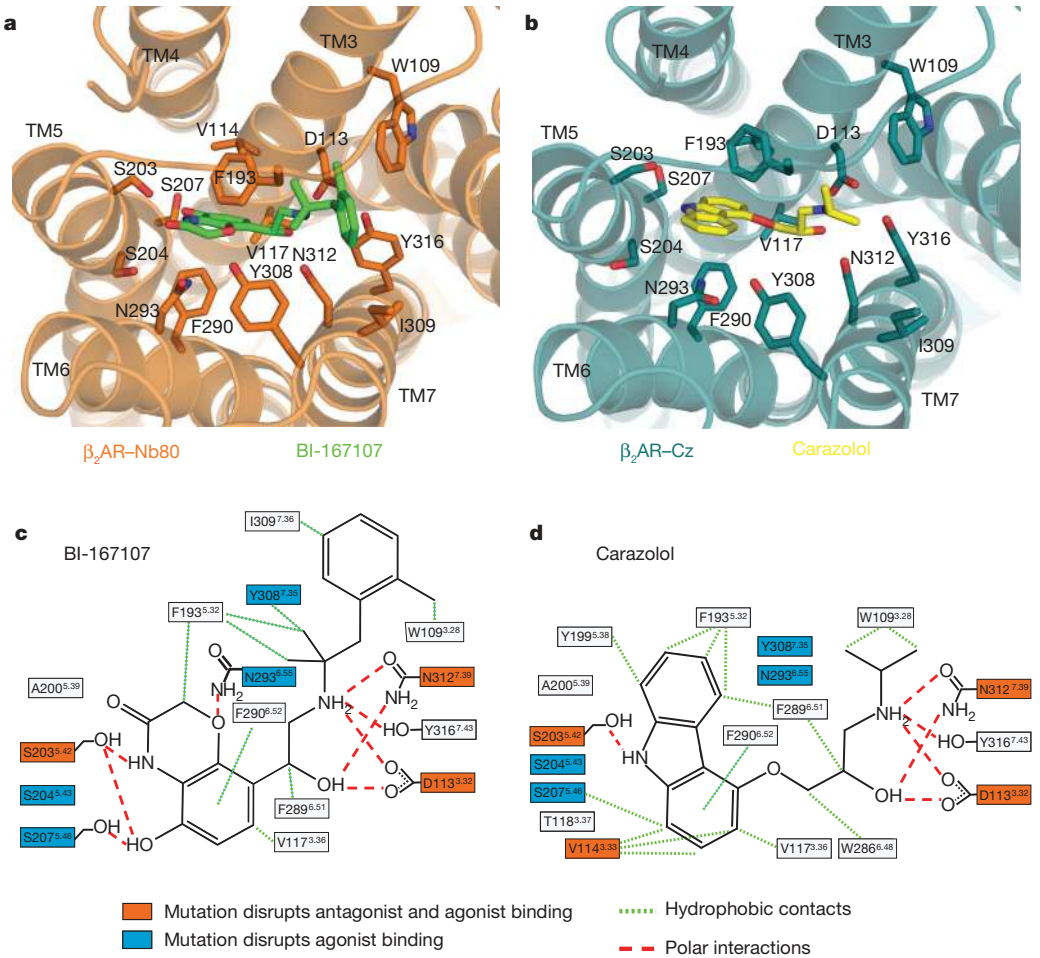

Figure 3 | Ligand binding pocket of BI-167107 and carazolol-bound β_2AR structures. **a**, **b**, Extracellular views of the agonist BI-167107-bound (**a**) and carazolol-bound (**b**) structures, respectively. Residues within 4 Å of one or both ligands are shown as sticks. In all panels, red and blue represent oxygen and nitrogen, respectively. **c**, **d**, Schematic representation of the interactions between the β_2AR and the ligands BI-167107 (**c**) and carazolol (**d**). The residues shown here have at least one atom within 4 Å of the ligand in the crystal structures. Mutations of amino acids in orange boxes have been shown to disrupt both antagonist and agonist binding. Mutations of amino acids in blue boxes have been shown to disrupt agonist binding. Green lines indicate potential hydrophobic interactions and orange lines indicate potential polar interactions.

agonist has a longer alkyl substituent on the amine, which ends with a phenyl ring that lies in a hydrophobic pocket formed by Trp 109$^{3.28}$, Phe 193$^{5.32}$ and Ile 309$^{7.36}$.

The greatest difference between inactive and active structures in the ligand-binding site is an inward bulge of TM5 centred around Ser 207$^{5.46}$, whose Cα position shifts by 2.1 Å (Fig. 4a). In addition, there are smaller inward movements of TM6 and TM7. The basal activity shown by the β_2AR indicates that the protein structure surrounding the binding pocket is relatively dynamic in the absence of ligand, such that it samples active and inactive conformations. The presence of Pro 211$^{5.50}$ in the following turn, which cannot form a hydrogen bond with the backbone at Ser 207$^{5.46}$, is likely to lower the barrier to the transition between the conformations observed in the presence of carazolol and BI-167107. There are extensive interactions between the carbonyl oxygen, amine and hydroxyl groups on the heterocycle of BI-167107 and Ser 203$^{5.42}$ and 207$^{5.46}$ in TM5, as well as Asn 293$^{6.55}$ in TM6 and Tyr 308$^{7.35}$ in TM7. In contrast, there is only one polar interaction between the nitrogen in the heterocycle of carazolol and Ser 203$^{5.42}$. Interactions of Ser 203$^{5.42}$, Ser 204$^{5.43}$ and Ser 207$^{5.46}$ with catecholamine hydroxyls have been proposed, on the basis of mutagenesis studies showing that these serines are important for agonist binding and activation[18,19]. Whereas Ser 204$^{5.43}$ does not interact directly with the ligand, it forms a hydrogen bond with Asn 293$^{6.55}$ on TM6, which is in turn linked to Tyr 308$^{7.35}$ of extracellular loop 3 (ECL3) (Fig. 3a). This tyrosine packs against Phe 193$^{5.32}$ of ECL2, and both residues move to close off the ligand-binding site from the extracellular space.

Asn 293$^{6.55}$ contributes to enantiomeric selectivity for catecholamine agonists[20]. The β-OH of BI-167107 does not interact with Asn 293$^{6.55}$, but forms hydrogen bonds with Asp 113$^{3.32}$ and Asn 312$^{7.39}$, similar to what is observed for carazolol in the inactive structure. The chirality of the β-OH influences the spatial position of the aromatic ring system in β_2AR ligands, so the effect of Asn 293$^{6.55}$ on β-OH enantiomeric selectivity may arise from its direct interaction with the aromatic ring system of the ligand, as well as its positioning of Ser 204$^{5.43}$ and Tyr 308$^{7.35}$, which also interact with this portion of the ligand. However, BI-167107 is not a catecholamine, and it is possible that the β-OH of catecholamine agonists, such as adrenaline and noradrenaline, has a direct interaction with Asn 293$^{6.55}$, because mutation of Asn 293$^{6.55}$ has a stronger influence on the preference for the chirality of the β-OH of catecholamine agonists, compared with non-catechol agonists and antagonists[20].

Trp $^{6.48}$ is highly conserved in Family A GPCRs, and it has been proposed that its rotameric state has a role in GPCR activation (rotamer toggle switch)[21]. We observe no change in the side chain rotamer of Trp 286$^{6.48}$ in TM6 (Fig. 4a), which lies near the base of the ligand-binding pocket, although its position shifts slightly in concert with rearrangements of nearby residues Ile 121$^{3.40}$ and Phe 282$^{6.44}$. Although there is spectroscopic evidence for changes in the environment of Trp $^{6.48}$ upon activation of rhodopsin[22], a rotamer change is not observed in the crystal structures of rhodopsin and low-pH opsin. Moreover, recent mutagenesis experiments on the serotonin 5HT4 receptor demonstrate that Trp $^{6.48}$ is not required for activation of this receptor by serotonin[23]. These observations indicate that, although changes in hydrophobic packing alter the conformation of the receptor in this region, changes in the Trp $^{6.48}$ rotamer do not occur as part of the activation mechanism.

It is interesting to speculate how the small changes around the agonist-binding pocket are coupled to much larger structural changes in the cytoplasmic regions of TMs 5, 6 and 7 that facilitate binding of Nb80 and Gs. A potential conformational link is shown in Fig. 4. Agonist interactions with Ser 203$^{5.42}$ and 207$^{5.46}$ stabilize a receptor conformation that includes a 2.1-Å inward movement of TM5 at position 207$^{5.46}$ and 1.4-Å inward movement of the conserved Pro 211$^{5.50}$ relative to the inactive, carazolol-bound structure. In the inactive state, the relative positions of TM5, TM3, TM6 and TM7 are stabilized by interactions between Pro 211$^{5.50}$, Ile 121$^{3.40}$, Phe 282$^{6.44}$ and Asn 318$^{7.45}$. The position of Pro 211$^{5.50}$ observed in the agonist structure is incompatible with this network of interactions, and Ile 121$^{3.40}$ and Phe 282$^{6.44}$ are repositioned, with a rotation of TM6 around Phe 282$^{6.44}$ leading to an outward movement of the cytoplasmic end of TM6.

Although some of the structural changes observed in the cytoplasmic ends of transmembrane domains of the β_2AR–T4L–Nb80 complex arise from specific interactions with Nb80, the fact that Nb80 and Gs induce or stabilize similar structural changes in the β_2AR, as determined by fluorescence spectroscopy and by agonist binding affinity, suggests that Nb80 and Gs recognize similar agonist-stabilized conformations. The observation that the transmembrane domains of rhodopsin and the β_2AR undergo similar structural changes upon activation provides further support that the agonist-bound β_2AR–T4L–Nb80 represents an active conformation and is consistent with a conserved mechanism of G protein activation.

However, the mechanism by which agonists induce or stabilize these conformational changes likely differs for different ligands and for different GPCRs. The conformational equilibria of rhodopsin and β_2AR differ, as shown by the fact that rhodopsin appears to adopt a fully active conformation in the absence of a G protein[24] whereas β_2AR cannot[15]. Thus, the energetics of activation and conformational

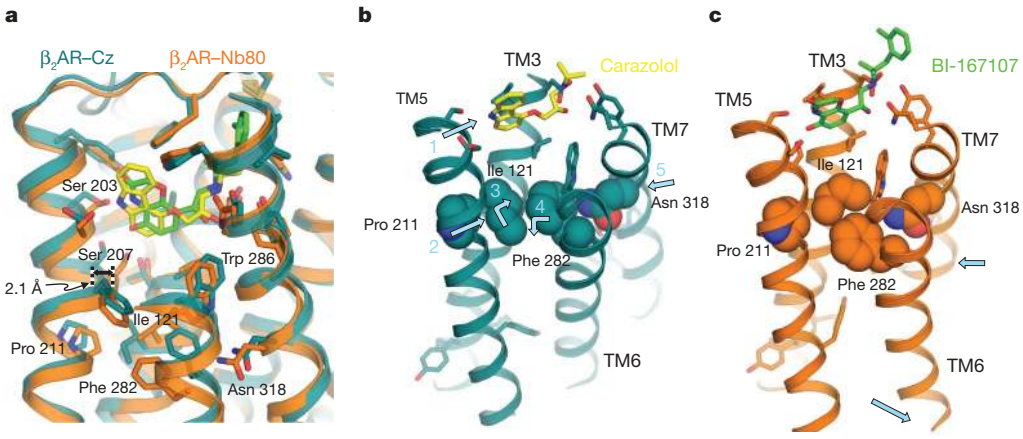

Figure 4 | Rearrangement of transmembrane segment packing interactions upon agonist binding **a**, The BI-167107- and carazolol-bound structures are superimposed to show structural differences propagating from the ligand-binding pocket. BI-167107 and carazolol are shown in green and yellow, respectively. **b**, Packing interactions that stabilize the inactive state are observed between Pro 211 in TM5, Ile 121 in TM3, Phe 282 in TM6 and Asn 318 in TM7. **c**, The inward movement of TM5 upon agonist binding destabilizes the packing of Ile 121 and Pro 211, resulting in a rearrangement of interactions between Ile 121 and Phe 282. These changes contribute to a rotation and outward movement of TM6 and an inward movement of TM7.

sampling can differ among different GPCRs, which likely gives rise to the variety of ligand efficacies displayed by these receptors. An agonist need only disrupt one key intramolecular interaction needed to stabilize the inactive state, as constitutive receptor activity can result from single mutations of amino acids from different regions of GPCRs[25]. Thus, disruption of these stabilizing interactions either by agonists or mutations lowers the energy barrier separating inactive and active states and increases the probability that a receptor can interact with a G protein.

METHODS SUMMARY

Crystallization. Preparation of β_2AR–T4L and Nb80 are described in Methods. BI-167107-bound β_2AR–T4L and Nb80 preincubated in 1:1.2 molar ratio were mixed in monoolein containing 10% cholesterol in 1:1.5 protein to lipid ratio (w/w). Initial crystallization leads were identified and optimized in 24-well glass sandwich plates using 50 nl protein:lipid drops overlaid with 0.8 µl precipitant solution in each well and sealed with a glass cover slip. Crystals for data collection were grown at 20 °C in hanging-drop format using 0.8 µl reservoir solution (36 to 44% PEG 400, 100 mM Tris pH 8.0, 4% DMSO, 1% 1,2,3-heptanetriol) diluted two- to fourfold in water. Crystals grew to full size, typically $40 \times 5 \times 5\ \mu m^3$, within 7 to 10 days. Crystals were flash-frozen and stored in liquid nitrogen with reservoir solution as cryoprotectant. Diffraction data collection and processing, and structure solution and refinement are described in Methods.

Full Methods and any associated references are available in the online version of the paper at www.nature.com/nature.

Received 6 July; accepted 1 November 2010.

1. Rosenbaum, D. M., Rasmussen, S. G. & Kobilka, B. K. The structure and function of G-protein-coupled receptors. *Nature* **459,** 356–363 (2009).
2. Scheerer, P. *et al.* Crystal structure of opsin in its G-protein-interacting conformation. *Nature* **455,** 497–502 (2008).
3. Park, J. H., Scheerer, P., Hofmann, K. P., Choe, H. W. & Ernst, O. P. Crystal structure of the ligand-free G-protein-coupled receptor opsin. *Nature* **454,** 183–187 (2008).
4. Li, J., Edwards, P. C., Burghammer, M., Villa, C. & Schertler, G. F. Structure of bovine rhodopsin in a trigonal crystal form. *J. Mol. Biol.* **343,** 1409–1438 (2004).
5. Palczewski, K. *et al.* Crystal structure of rhodopsin: a G protein-coupled receptor. *Science* [see comments] **289,** 739–745 (2000).
6. Vogel, R. & Siebert, F. Conformations of the active and inactive states of opsin. *J. Biol. Chem.* **276,** 38487–38493 (2001).
7. Rosenbaum, D. M. *et al.* GPCR engineering yields high-resolution structural insights into β-adrenergic receptor function. *Science* **318,** 1266–1273 (2007).
8. Rasmussen, S. G. *et al.* Crystal structure of the human β_2 adrenergic G-protein-coupled receptor. *Nature* **450,** 383–387 (2007).
9. Cherezov, V. *et al.* High-resolution crystal structure of an engineered human β_2-adrenergic G protein-coupled receptor. *Science* **318,** 1258–1265 (2007).
10. Hanson, M. A. *et al.* A specific cholesterol binding site is established by the 2.8 Å structure of the human β_2-adrenergic receptor. *Structure* **16,** 897–905 (2008).
11. Warne, T. *et al.* Structure of a β_1-adrenergic G-protein-coupled receptor. *Nature* **454,** 486–491 (2008).
12. Jaakola, V. P. *et al.* The 2.6 Angstrom crystal structure of a human A_{2A} adenosine receptor bound to an antagonist. *Science* **322,** 1211–1217 (2008).
13. Ghanouni, P. *et al.* Functionally different agonists induce distinct conformations in the G protein coupling domain of the β_2 adrenergic receptor. *J. Biol. Chem.* **276,** 24433–24436 (2001).
14. Rosenbaum, D. M. *et al.* Structure and function of an irreversible agonist–β2 adrenoceptor complex. *Nature* doi:10.1038/nature09665 (this issue).
15. Yao, X. J. *et al.* The effect of ligand efficacy on the formation and stability of a GPCR-G protein complex. *Proc. Natl Acad. Sci. USA* **106,** 9501–9506 (2009).
16. Hamers-Casterman, C. *et al.* Naturally occurring antibodies devoid of light chains. *Nature* **363,** 446–448 (1993).
17. Ballesteros, J. A. & Weinstein, H. Integrated methods for the construction of three-dimensional models and computational probing of structure-function relations in G protein coupled receptors. *Meth. Neurosci.* **25,** 366–428 (1995).
18. Strader, C. D. *et al.* Identification of residues required for ligand binding to the β-adrenergic receptor. *Proc. Natl Acad. Sci. USA* **84,** 4384–4388 (1987).
19. Liapakis, G. *et al.* The forgotten serine. A critical role for Ser-$203^{5.42}$ in ligand binding to and activation of the β_2-adrenergic receptor. *J. Biol. Chem.* **275,** 37779–37788 (2000).
20. Wieland, K., Zuurmond, H. M., Krasel, C., Ijzerman, A. P. & Lohse, M. J. Involvement of Asn-293 in stereospecific agonist recognition and in activation of the beta 2-adrenergic receptor. *Proc. Natl Acad. Sci. USA* **93,** 9276–9281 (1996).
21. Shi, L. *et al.* β_2 adrenergic receptor activation. Modulation of the proline kink in transmembrane 6 by a rotamer toggle switch. *J. Biol. Chem.* **277,** 40989–40996 (2002).
22. Ahuja, S. & Smith, S. O. Multiple switches in G protein-coupled receptor activation. *Trends Pharmacol. Sci.* **30,** 494–502 (2009).
23. Pellissier, L. P. *et al.* Conformational toggle switches implicated in basal constitutive and agonist-induced activated states of 5-hydroxytryptamine-4 receptors. *Mol. Pharmacol.* **75,** 982–990 (2009).
24. Altenbach, C., Kusnetzow, A. K., Ernst, O. P., Hofmann, K. P. & Hubbell, W. L. High-resolution distance mapping in rhodopsin reveals the pattern of helix movement due to activation. *Proc. Natl Acad. Sci. USA* **105,** 7439–7444 (2008).
25. Parnot, C., Miserey-Lenkei, S., Bardin, S., Corvol, P. & Clauser, E. Lessons from constitutively active mutants of G protein-coupled receptors. *Trends Endocrinol. Metab.* **13,** 336–343 (2002).

Supplementary Information is linked to the online version of the paper at www.nature.com/nature.

Acknowledgements We acknowledge support from National Institutes of Health Grants NS028471 and GM083118 (B.K.K.), GM56169 (W.I.W.), P01 GM75913 (S.H.G), and P60DK-20572 (R.K.S.), the Mathers Foundation (B.K.K. and W.I.W.), the Lundbeck Foundation (Junior Group Leader Fellowship, S.G.F.R.), the University of Michigan Biomedical Sciences Scholars Program (R.K.S.), the Fund for Scientific Research of Flanders (FWO-Vlaanderen) and the Institute for the encouragement of Scientific Research and Innovation of Brussels (ISRIB) (E.P. and J.S.).

Author Contributions S.G.F.R. screened and characterized high affinity agonists, identified and determined dissociation rate of BI-167107, screened, identified and characterized MNG-3, performed selection and characterization of nanobodies, purified and crystallized the receptor with Nb80 in LCP, optimized crystallization conditions, grew crystals for data collection, reconstituted receptor in HDL particles and determined the effect of Nb80 and Gs on receptor conformation and ligand binding affinities, assisted with data collection and preparing the manuscript. H.-J.C. processed diffraction data, solved and refined the structure, and assisted with preparing the manuscript. J.J.F. expressed, purified, selected and characterized nanobodies, purified and crystallized receptor with nanobodies in bicelles, assisted with growing crystals in LCP, and assisted with data collection. E.P. performed immunization, cloned and expressed nanobodies, and performed the initial selections. J.S. supervised nanobody production. P.S.K. and S.H.G. provided MNG-3 detergent for stabilization of purified β_2AR. B.T.D. and R.K.S. provided ApoA1 and Gs protein, and reconstituted β_2AR in HDL particles with Gs. D.M.R. characterized the usefulness of MNG-3 for crystallization in LCP and assisted with manuscript preparation. F.S.T. expressed β_2AR in insect cells and with T.S.K performed the initial stage of β_2AR purification. A.P., A.S. assisted in selection of the high-affinity agonist BI-167107. I.K. synthesized BI-167,107. P.C. characterized the functional properties of BI-167,107 in CHO cells. W.I.W. oversaw data processing, structure determination and refinement, and assisted with writing the manuscript. B.K.K. was responsible for the overall project strategy and management, prepared β_2AR in lipid vesicles for immunization, harvested and collected data on crystals, and wrote the manuscript.

Author Information Coordinates and structure factors for β_2AR–Nb80 are deposited in the Protein Data Bank (accession code 3P0G). Reprints and permissions information is available at www.nature.com/reprints. The authors declare no competing financial interests. Readers are welcome to comment on the online version of this article at www.nature.com/nature. Correspondence and requests for materials should be addressed to B.K.K. (kobilka@stanford.edu) or W.I.W. (bill.weis@stanford.edu).

METHODS

Preparation of β2AR–T4L and nanobody-80 for crystallography. β2AR–T4L was expressed in Sf-9 insect cell cultures infected with β2AR–T4L baculovirus, and solubilized according to methods described previously[26]. Functional protein was obtained by M1 Flag affinity chromatography (Sigma) before and following alprenolol-Sepharose chromatography[26]. In the second M1 chromatography step, receptor-bound alprenolol was exchanged for high-affinity agonist BI-167107 and dodecylmaltoside was exchanged for the MNG-3 amphiphile (11,11-bis-β-D-maltopyranosidylmethyl-heneicosane, Supplementary Fig. 6, obtained from P. S. Chae and S. H. Gellman) for increased receptor stability. The agonist-bound and detergent-exchanged β2AR–T4L was eluted in 10 mM HEPES pH 7.5, 100 mM NaCl, 0.02% MNG-3 and 10 μM BI-167107 followed by removal of N-linked glycosylation by treatment with PNGaseF (NEB). The protein was concentrated to ~50 mg ml^{-1} with a 100 kDa molecular weight cut off Vivaspin concentrator (Vivascience).

Nanobody-80 (Nb80) bearing a carboxy-terminal His_6 tag was expressed in the periplasm of *Escherichia coli* strain WK6 following induction with IPTG. Cultures of 0.6 l were grown to $A_{600} = 0.7$ at 37 °C in TB media containing 0.1% glucose, 2 mM $MgCl_2$, and 50 μg ml^{-1} ampicillin. Induced cultures were grown overnight at 28 °C. Cells were harvested by centrifugation and lysed in ice-cold buffer (50 mM Tris pH 8.0, 12.5 mM EDTA and 0.125 M sucrose), then centrifuged to remove cell debris. Nb80 was purified by nickel affinity chromatography, dialysed against buffer (10 mM HEPES pH 7.5, 100 mM NaCl), and spin concentrated to ~120 mg ml^{-1}.

Crystallization. BI-167107 bound β2AR–T4L and Nb80 were mixed in 1:1.2 molar ratio, incubated 2 h at room temperature before mixing with liquefied monoolein (M7765, Sigma) containing 10% cholesterol (C8667, Sigma) in 1:1.5 protein to lipid ratio (w/w) using the twin-syringe mixing method reported previously[27]. Initial crystallization leads were identified using in-house screens and optimized in 24-well glass sandwich plates using 50 nl protein:lipid drops manually delivered and overlaid with 0.8 μl precipitant solution in each well and sealed with a glass cover slip. Crystals for data collection were grown at 20 °C by hanging drop vapour diffusion using 0.8 μl reservoir solution (36 to 44% PEG 400, 100 mM Tris pH 8.0, 4% DMSO, 1% 1,2,3-heptanetriol) diluted two- to fourfold in Milli-Q water. Crystals grew to full size within 7 to 10 days. Crystals were flash-frozen and stored in liquid nitrogen with reservoir solution as cryoprotectant.

Microcrystallography data collection and processing. Diffraction data were measured at beamline 23-ID of the Advanced Photon Source, using a 10-μm diameter beam. Low dose 1.0° rotation images were used to locate and centre crystals for data collection. Data were measured in 1.0° frames with exposure times typically 5–10 s with a 5× attenuated beam. Only 5–10° of data could be measured before significant radiation damage occurred. Data were integrated and scaled with the HKL2000 package[28].

Structure solution and refinement. Molecular replacement phases were obtained with the program Phaser[29]. The search models were (1) the high-resolution carazolol-bound β_2AR structure, PDB ID 2RH1, but with T4L and all water, ligand and lipid molecules removed) and a nanobody (PDB ID 3DWT, water molecules removed) as search models. The rotation and translation function *Z* scores were 8.7 and 9.0 after placing the β_2AR model, and the nanobody model placed subsequently had rotation and translation function *Z* scores of 3.5 and 11.5. The model was refined in Phenix[30] and Buster[31], using a group B factor model with one B for main chain and one B for side chain atoms. Refinement statistics are given in Supplementary Table 2. Despite the strong anisotropy (Supplementary Table 2), the electron density was clear for the placement of side chains.

Ligand binding on receptor reconstituted in HDL particles. The effect of Nb80 and Gs on the receptors affinity for agonists was compared in competition binding experiments. The β_2AR and β_2AR–T4L (both truncated at position 365) purified as previously described[7,8] were reconstituted in high-density lipoprotein (HDL) particles followed by reconstitution of Gs into HDL particles containing β_2AR according to previously published methods[32]. [^{3}H]-dihydroalprenolol ([^{3}H]-DHA; 0.6 nM) was used as radioligand and agonist (−)-isoproterenol (ISO) or inverse agonist ICI-118,551 (ICI) as competitor. Nb80 was used at 1 μM. GTPγS was used at 10 μM. TBS (50 mM Tris pH 7.4, 150 mM NaCl) containing 0.1% BSA was used as binding buffer. Bound [^{3}H]-DHA was separated from unbound on a Brandel harvester by passing over a Whatman GF/B filter (presoaked in TBS with 0.3% polyethylenimine) and washed in cold TBS. Radioligand binding was measured in a Beckman LS6000 scintillation counter. Ligand binding affinity (K_d) of DHA was determined from saturation binding curves using GraphPad Prism software. Normalized ISO competition binding data were fit to a two-site competition binding model by using GraphPad Prism. Binding affinities of ISO (K_i values, tabulated in Supplementary Table 1) were determined from 50% inhibitory concentration (IC_{50}) values using the equation $K_i = IC_{50}/(1 + [L]/K_d)$.

cAMP assay. To determine the functional potency of BI-167107, changes in intracellular cAMP levels were determined with CHO-hβ_2AR cells in suspension (15,000 cells per well) by using Alphascreen technology (PerkinElmer Life and Analytical Sciences) and a 384-well plate format (Optiplate; PerkinElmer Life and Analytical Sciences), according to the manufacturer's protocol. In brief, cells were stimulated with the respective agonists at different concentrations in Hanks' buffered saline solution supplemented with 5 mM HEPES, 0.1% bovine serum albumin and 500 mM 3-isobutyl-1-methylxanthine for 30 min at room temperature. Cells were lysed by using Alphascreen reagents. After 2 h, plates were read on an Envision plate reader (PerkinElmer Life and Analytical Sciences). The concentration of cAMP in the samples was calculated from a standard curve.

Bimane fluorescence spectroscopy on β_2AR reconstituted in HDL particles. To compare the effects on receptor conformation of Gs and Nb80 binding the purified β_2AR was labelled with the environmentally sensitive fluorescent probe monobromobimane (Invitrogen) at cysteine 265 located in the cytoplasmic end of TM6, and reconstituted into HDL particles (mBB-β_2AR/HDL). Prior to obtaining fluorescence emission spectra, 10 nM mBB-β_2AR/HDL was incubated 30 min at room temperature in buffer (20 mM HEPES pH 7.5, 100 mM NaCl) in the absence or presence of 10 μM ISO, 1 μM ICI, 300 nM Gs heterotrimer, or 300 nM Nb80, or in combinations of ISO with Gs, ISO with Nb80, and ICI with Nb80. Fluorescence spectroscopy was performed on a Spex FluoroMax-3 spectrofluorometer (Jobin Yvon) with photon-counting mode, using an excitation and emission bandpass of 5 nm. Excitation was set at 370 nm and emission was collected from 415 to 535 nm in 1-nm increments with 0.3 s nm^{-1} integration time. Fluorescence intensity was corrected for background fluorescence from buffer and ligands. The curves shown in Fig. 1b and c are each the average of triplicate experiments.

High affinity β_2AR agonist screening by bimane fluorescence spectroscopy. To obtain high affinity agonist candidates with slow dissociation rates for crystallography, a screening process of commercially available drugs and compound libraries from medicinal and biotech industry was initiated. Screening was conducted in several rounds on more than 50 compounds. Each compound (10 μM) was incubated with 100 nM purified mBB-β_2AR in DDM buffer (20 mM HEPES pH 7.5, 100 mM NaCl, 0.1% dodecylmaltoside (DDM)) for 30 min at room temperature before emission scanning, using same equipment and settings as described in the section above. Compounds inducing the largest red shift in λ_{max} and decrease in bimane fluorescence emission were identified. Closely related structural analogues were subsequently screened using same criteria for selection. Several lead candidate compounds were then subjected to dissociation experiments to identify the agonist with the slowest rate of dissociation. In these experiments, 100 nM mBB-β_2AR was incubated with 1 μM lead compound in DDM buffer for 2 h at room temperature before obtaining the emission scan at $t = 0$ (example in Supplementary Fig. 2d, green spectra). An excess amount (200 μM) of the neutral antagonist alprenolol (ALP) was added to identical samples followed by measurement of bimane emission at various time points in a period up to 7 days or until complete dissociation of agonist.

26. Kobilka, B. K. Amino and carboxyl terminal modifications to facilitate the production and purification of a G protein-coupled receptor. *Anal. Biochem.* **231,** 269–271 (1995).
27. Caffrey, M. & Cherezov, V. Crystallizing membrane proteins using lipidic mesophases. *Nature Protocols* **4,** 706–731 (2009).
28. Otwinowski, Z. & Minor, W. Processing of X-ray diffraction data collected in oscillation mode. *Methods Enzymol.* **276,** 307–326 (1997).
29. McCoy, A. J. *et al. Phaser* crystallographic software. *J. Appl. Cryst.* **40,** 658–674 (2007).
30. Afonine, P. V., Grosse-Kunstleve, R. W. & Adams, P. D. A robust bulk-solvent correction and anisotropic scaling procedure. *Acta Crystallogr. D* **61,** 850–855 (2005).
31. Blanc, E. *et al.* Refinement of severely incomplete structures with maximum likelihood in *BUSTER-TNT*. *Acta Crystallogr. D* **60,** 2210–2221 (2004).
32. Whorton, M. R. *et al.* A monomeric G protein-coupled receptor isolated in a high-density lipoprotein particle efficiently activates its G protein. *Proc. Natl Acad. Sci. USA* **104,** 7682–7687 (2007).